ChemComm

COMMUNICATION

View Article Online
View Journal | View Issue

Cite this: *Chem. Commun.*, 2017, 53, 4826

Received 13th January 2017,
Accepted 30th March 2017

DOI: 10.1039/c7cc00310b

rsc.li/chemcomm

DNA-spheres decorated with magnetic nanocomposites based on terminal transfer reactions for versatile target detection and cellular targeted drug delivery†

Yingshu Guo,[ab] Yujie Wang,[ab] Shuang Li,[ac] Li Niu,[a] Di Wei[ad] and Shusheng Zhang *[a]

We present an elegant approach to make a magnetic nanoparticle (MNP) conjugated DNA-sphere (MNP/DNA-SP) which is integrated with disulfide (MNP/DS-SP) or an aptamer (MNP/sgc8-SP) for GSH detection, selective cancer cell recognition, effective drug delivery, and bioimaging.

Deoxyribose nucleic acid (DNA) complementarity is achieved by distinguishing interactions in four nucleobases: cytosine (C), thymine (T), adenine (A) and guanine (G). In nature, the fundamentals of DNA replication and transcription are complementary. This process is made possible by the inherent characteristics of the two DNA strands; when they are aligned antiparallel to each other, the nucleotide bases at each position in the sequences will be complementary. They will be so alike that it will be like looking in the mirror. The traditional view of DNA was its role as an inheritable molecule. Recently, numerous successful conceptions of DNA as a genetic and a generic material to merge the burgeoning fields of biology and nanotechnology have been developed.[1] A hydrogel was constructed using actual genes as monomers and DNA as crosslinkers. The gel scaffolding was incorporated with the genes; thereby, a protein-producing hydrogel was constructed.[2] A method for preparing DNA nanocages was developed, which could effectively encapsulate enzymes with high profit. On the basis of encapsulation, 5 of 6 detected metabolic enzymes performed 4–10 times higher than the free enzyme on turnover numbers.[3] DNA nanoflowers were built to selectively recognize cancer cells and deliver anticancer drugs to the target.[4] Collectively, all those strategies have shown very intriguing performances. However, these approaches have the intrinsic drawback of inconvenient bioseparation. Therefore, the latest progress in nanotechnology reinforces the prospect of novel materials for the toilless purifications and separations of biomolecules, which are of great importance in biomedical applications. The magnetic nanovector was a good candidate, which is illustrated by its rapid response to magnetic fields.[5]

Magnetic particles, as remarkable materials, have been broadly applied for diagnosis and treatment in biology.[6] Magnetic nanovectors have both the properties of magnetic nanoparticles and imported materials, and extend the fields of magnetic materials.[7] Due to convenient manipulation, such as simple, efficient magnetic separation and recycling, numerous researchers have shown interest in carrier, adsorption and enrichment.[8] Besides, great efforts have been devoted to magnetic resonance imaging (MRI) due to its high spatial resolution and tissue penetration.[9] Compared with the traditional methods, these experimental results show a greater advantage on the sensitivity and selectivity.

In medical diagnosis, 'false positive' results may be obtained due to the determination of a single target in a disease associated with multifarious biomolecules.[10] A traditional single detection method can never meet the requirements. The accuracy of early disease diagnosis could be efficaciously enhanced by detecting diversiform targets. A variety of platforms for the determination of multi-targets have been established in the biomedical field.[11] Multipurpose materials and technologies at the concordance of bioimaging and sensing are intriguing problems in multi-target detection.[12] Compared to traditional single-function nanoparticles, multifunctional nanovectors reveal huge potential for optimized therapy of personalized medicine due to their properties of multi-function, for instance, biosensing, targeting, drug delivery, and therapy.[13]

As an isothermal replication technique of DNA, rolling circle amplification (RCA) has performed excellently for highly sensitive detection of proteins and the targeting of nucleic acids.[14] In most assays at the base of RCA, the quantification of the

[a] *Shandong Province Key Laboratory of Detection Technology for Tumor Makers, School of Chemistry and Chemical Engineering, Linyi University, Linyi 276005, China. E-mail: shushzhang@126.com*
[b] *College of Chemistry, Chemical Engineering and Materials Science, Collaborative Innovation Center of Functionalized Probes for Chemical Imaging in Universities of Shandong, Key Laboratory of Molecular and Nano Probes, Ministry of Education, Shandong Normal University, Jinan 250014, China*
[c] *Shandong Provincial Key Laboratory of Life-Organic Analysis, College of Chemistry and Chemical Engineering, Qufu Normal University, Qufu, 273165, China*
[d] *Nokia Research Center, Broers Building, 21 J. J. Thomson Avenue, Cambridge, UK*

† Electronic supplementary information (ESI) available: Summary of oligonucleotide sequences; Fig. S1–S9; and Tables S1 and S2. See DOI: 10.1039/c7cc00310b

target is realized through the RCA product quantification. The RCA products not only turn into nanostructures by self-assembly, but they also form solubilized threads.[15] By designing rational DNA synthetic methods to generate nanostructures, DNA structures (DNA-sphere, DNA-SP) that contain predetermined sequences were obtained by RCA in this paper. Anticancer drug doxorubicin (DOX) has priority in combination with double-stranded 5′-GC-3′ or 5′-CG-3′, leading to the quenching of drug fluorescence.[16] DNA-SP was projected for the sequences that would constitute combination sites of DOX. DNA-SP provided drug-loading sites for doxorubicin (DOX). Stochastically, unloading DOX from internalized DNA-SP is a simple diffusion promoted by intracellular factors, for example, nuclease degradation, pH, and an ionic environment.[17] The primers of the RCA reaction were biotinylated at the 5′-end, and DNA-SP can be easily bound to streptavidin modified magnetic nanoparticles (MNPs) *via* biotin–streptavidin specific recognition to perform the following magnetic separation. MNP/DNA-SP may be imported for delivery of drugs and imaging applications. However, normal cells can internalize MNP/DNA-SP *via* the endocytosis process. In this study, the normal cells will be unavoidably hurt by the drugs due to some unanticipated uptake. Hence, it is an imperious demand to facilitate an efficient way for promoting the recognition of cancer cells and selectively bind them to abnormal cells. As a proof of concept, aptamer sgc8, which can bind to target (CEM) cells but not to nontarget cells,[18] was contained in DNA-SP by a carefully designed sequence called the sgc8-tethered DNA-sphere (sgc8-SP). A sgc8-SP decorated magnetic nanovector (MNP/sgc8-SP) was developed for target CEM cells (Fig. 1).

Terminal deoxynucleotidyl transferase (TdT) catalyzed the condensation of deoxyribonucleotides on 3′-hydroxyl ends of DNA strands in a template-independent manner.[19] TdT-mediated adenine (A)-tailing covalently attached to DNA-SP allowed sequencing from the 3′-ends. And then, the (T) tailing sequence of the 3′-end was hybridized to the poly(A)-tailed DNA-SP. The use of a 5′-end of poly(T)-tailed sequence can achieve specific recognition and delivery goals for other targets. This strategy could be applied to a target that has not found its aptamer. To verify the universal feasibility of MNP/DNA-SP as targeted recognition and delivery vectors, another poly(T) tailed DNA sequence was selected as the targeting recognition molecule. As a proof of concept, a poly(T) tailed sequence with folic acid (FA) modified at the 5′-end was conjugated to MNP/DNA-SP by means of A–T hybridization to form FA decorated MNP/DNA-SP (MNP/FA-SP) (Fig. 2). The FA can bond in high affinity with its ligand so that the folate receptor (FR) of the cell surface, which is overexpressed in some cancer cells up to 100–300 times higher than normal cells, can be a significant tumour marker.[20] So MNP/FA-SP combined targeting with an FR of a cancer cell surface results in the delivery of drugs to cancer

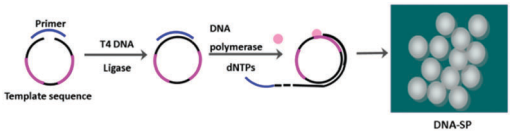

Fig. 1 Schematic diagram of DNA-SP.

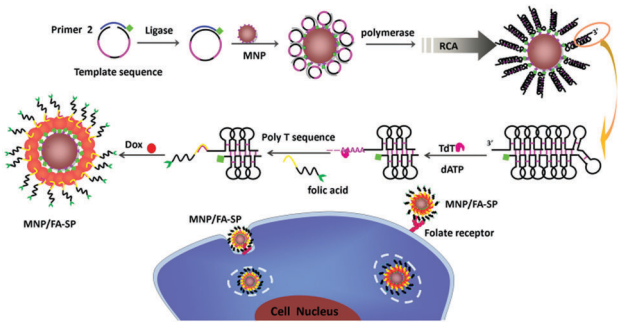

Fig. 2 Schematic diagram of folic acid decorated MNP/DNA-SP for cellular targeted drug delivery.

cells. To achieve multi-functionalization responsiveness, we incorporated disulfide linkages into RCA primers, and MNP/DNA-SP that contained disulfide (MNP/DS-SP) was obtained by RCA (Fig. 3). Disulfide can be cleaved by a reduced biothiol (for example, glutathione, GSH) and DNA-SP was released. Strong DOX fluorescence signals were used for GSH detection. By incorporating aptamers, folic acid (FA), disulfide linkages, and DOX into the magnetic nanovector, the synthesized MNP/DNA-SP can be used for GSH detection and stimuli-responsive drug therapy.

Our study of a specific reduced thiol probe (MNP/DS-SP) is expounded in Fig. 3. Once in the reduced thiol solution, the disulfide bond experienced disulfide cleavage *via* reaction with reduced thiols. After magnetic separation, DOX will be released, which will be convenient for detecting changes in fluorescence. The capability of a MNP/DS-SP sensing ensemble for the quantitative detection of reduced thiols was evaluated and successful (here, GSH was chosen as the model). Fig. 4 shows the fluorescence spectral changes on the spot of different GSH concentrations. The emission intensity of the 595 nm band increased remarkably as the GSH concentration increased. Additionally, there was a good linearity between the relative fluorescence intensity and the concentrations of GSH in the range of 2.0×10^{-9} to 8.0×10^{-8} M. The linear regression equations were received as $Y = 49.1X + 77.3$ (Y represents the relative fluorescence intensity, X represents the concentration of GSH, 10^{-8} M, $n = 9$, $R = 0.996$). The reproducibility of the method was tested with 11 serial tests of 5.0×10^{-9} M GSH. The relative standard deviation (RSD) was calculated to be 3.5%,

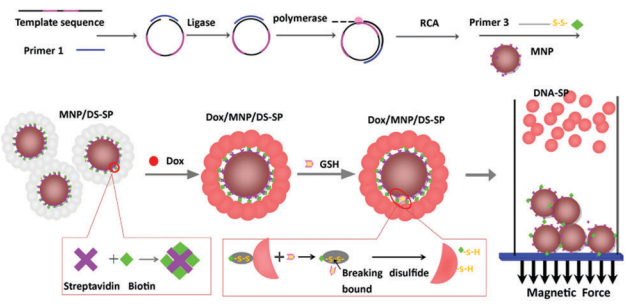

Fig. 3 Schematic diagram of disulfide decorated MNP/DNA-SP for GSH detection.

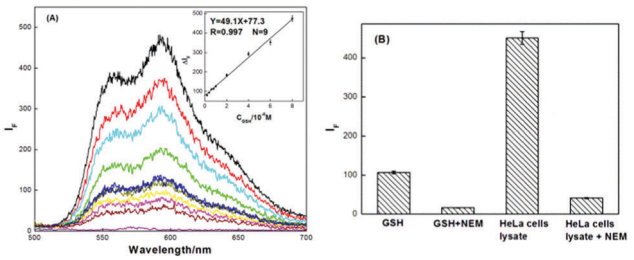

Fig. 4 (A) Fluorescence emission spectra of DOX with different concentrations of GSH (from bottom to top: 0, 1.0×10^{-9}, 2.0×10^{-9}, 4.0×10^{-9}, 6.0×10^{-9}, 8.0×10^{-9}, 1.0×10^{-8}, 2.0×10^{-8}, 4.0×10^{-8}, 6.0×10^{-8}, 8.0×10^{-8} M); inset: fluorescence emission intensity of DOX at 595 nm as a function of the GSH concentration, the magnitude of the error bars was calculated by three independent measurements. (B) Comparison of the fluorescence intensities of 5.0×10^{-9} M GSH solution, GSH treated with NEM, HeLa cell lysate and HeLa cell lysate treated with NEM.

which makes it clear that this developed method has a good reproducibility.

To gain more insight into the reaction between reduced thiols and MNP/DS-SP, we treated the sample with 1.0 mM of *N*-ethylmaleimide (NEM) for 60 min to block the thiol[21] followed by addition of the pretreated sample to MNP/DS-SP, and we recorded the fluorescence intensity. Much smaller fluorescence increments were obtained (Fig. 4B), proving that the mercapto group is indispensable to detection. Based on these results, we were also able to confirm that the release of MNP/DS-SP occurred in response to the reduced thiol.

To affirm the applicability of the developed method in biological samples, we applied it to the extracts of Ramos cells to detect intracellular reduced thiols. The concentration of intracellular reduced thiols was ~3.705 fmol per cell. To verify analytical recovery, different concentrations of GSH were added to cell lysate dilution samples containing different concentrations of GSH before and after being assayed. The laboratory findings of these recovery tests are also shown in Table S2 (ESI†). These results show a high reliability for this assay.

Our approach to a cell-specific probe is illustrated as follows. It involves the aptamer system that, we suggest, will be selectively recognized by CEM cells *via* sgc8-mediated endocytosis. Once in the cell, it will release DOX and lead to fluorescence changes that can be easily monitored. MNP/sgc8-SP will specifically bind to the target CEM cells, rather than to non-target Ramos cells. The binding ability was confirmed by flow-cytometric analysis (Fig. S5A and B, ESI†), verifying that a base for MNP/sgc8-SP was guided in the action of the aptamer moiety toward the target location. In CEM cells treated with DOX-loaded MNP/sgc8-SP for 24 h, DOX was found to accumulate in the nucleus (Fig. S5C, ESI†). The distribution of DOX in the cell nucleus is inferred to give rise to the tardy release of DOX.[22] The biocompatibility of MNP/sgc8-SP was verified by a cytotoxicity assay. After incubation with MNP/sgc8-SP, both the CEM cell and Ramos cell showed high cell viability (above 90%) (Fig. S5D, ESI†), verifying that our drug delivery system has excellent biocompatibility. The results confirm that these MNP/sgc8-SPs have potential application as fluorescently traceable drug carriers.

Furthermore, selective cytotoxicity was shown from the cytotoxicity assay results, which displayed that DOX was delivered by MNP/sgc8-SP in nontarget Ramos cells much more substantially than in target CEM cells. The nonselective cytotoxicity of free DOX is simultaneously contrasting in both Ramos and CEM cells (Fig. S6, ESI†). The capability of targeted drug delivery is indicated by the selective cytotoxicity of DOX delivered by MNP/sgc8-SP.

When a target has not been screened, its aptamer, a structure like MNP/sgc8-SP, is no longer practicable. Certain different ligands can target specific species. TdT-mediated poly A-tailing covalently attached to DNA-SP allowed sequencing from 3′-ends. Then, a poly T tailing sequence of the 3′-end was hybridized to the poly A-tailed DNA-SP. A 5′-end of the poly T tailed sequence can be used to functionalize specific recognition and delivery goals for those targets. Significantly, the FR is overexpressed in some cancer cells. As a tumour marker, it can bond with its ligand FA, resulting in various targeted nanocarriers. This has been applied to imaging and therapeutics successfully.[23] FA as a model was chosen to accomplish this idea. To estimate whether the binding affinity and specificity between conjugated FA and FR on cell membranes is still preservative, the binding of DOX-loaded MNP/FA-SP toward HeLa cells and control cells (MCF-7 cell) was studied using flow cytometry. As we can see from Fig. S7A (ESI†), a significant shift was performed by HeLa cells treated with DOX-loaded MNP/FA-SP, but no large shift was performed by MCF-7 cells (Fig. S7B, ESI†). To further determine if DOX-loaded MNP/FA-SP could be used for specific labeling for live cells, MNP/FA-SPs with cells were incubated together. They were incubated at 4 °C and then washed. They were found to be specifically bound with each other, as shown in Fig. S7C (ESI†). DOX accumulation was discovered in the cell nucleus, whereas the HeLa cells were incubated with DOX-loaded MNP/FA-SP after 24 h. Because labeling with DOX-loaded MNP/FA-SP was specifically indicated, this approach can also be an extension for particular cell types or different proteins to view their interactions in the target simultaneously.

The therapeutic efficacy of *in vivo* drugs (DOX) delivered by this platform was evaluated through a model of CEM (or Ramos) on a mouse's subcutaneously xenografted tumour, which was developed by the subcutaneous injection of CEM cells (or Ramos cells) in the back of the bearing mice. Four groups of mice were divided for comparative efficacy studies in which the following regimens were administered by intravenous injections every other day: MNP/sgc8-SP or DOX-loaded MNP/sgc8-SP. One mouse from each group was chosen as a representative for taking photos. As can be seen in Fig. S9 (ESI†), after 12 days the tumour growth slowed down significantly for the DOX-loaded MNP/sgc8-SP subcutaneously treated CEM mouse (2); however, there was fast growth in the CEM mouse (1) treated subcutaneously with MNP/sgc8-SP. Compared with the Ramos mouse (3) subcutaneously treated with MNP/sgc8-SP, the Ramos mouse (4) subcutaneously treated with DOX-loaded MNP/sgc8-SP showed no significant inhibition of tumour growth. These results are attributed to the features of DOX-loaded MNP/sgc8-SP, which has the ability of unique recognition of macromolecular weight and

brought about, comparatively, a highly concentrated accumulation of drugs and prolonged the time of drug retention in the tumour. Overall, these results make DOX-loaded MNP/DNA-SP a development prospect for targeted theranostics to cancer.

In conclusion, we synthesized MNP/DNA-SP and DOX embedded in MNP/DNA-SP for drug carriers. By incorporating different functional elements, such as aptamers and disulfide linkages into different DNA-SPs, the synthesized MNP/DNA-SP can be used for targeted detection (*e.g.* GSH, CEM cells) and drug delivery, resulting in the relief of cell apoptosis in target cells. For those that have not yet been screened by their aptamers specifically, functional element (*e.g.* FA) modified poly T tailed sequences were taken to MNP/DNA-SP by terminal transferase mediated chain elongation. Different functional elements as ligands for different targets can be incorporated into MNP/DNA-SP, which achieves versatile targeted applications. The advantages of MNP/DNA-SP include good selectivity, superior biocompatibility and convenient drug delivery. The potent antitumor efficacy of drugs delivered by the biocompatible MNP/DNA-SP was tested in a model of xenografted tumours of mice. Thus, the result is a combination of traceable targeted detection and drug delivery that serves as a multifunctional MNP/DNA-SP, which will provide a novel platform for target detection and versatile biomedical applications.

This work was supported by the National Natural Science Foundation of China (21575056, 21535002), the Natural Science Foundation of Shandong Province of China (ZR2016JL010), and the Program for New Century Excellent Talents in University of Ministry of Education of China (NCET-13-0845).

Notes and references

1 (*a*) S. H. Um, J. B. Lee, N. Park, S. Y. Kwon, C. C. Umbach and D. Luo, *Nat. Mater.*, 2006, **5**, 797–801; (*b*) J. B. Lee, J. Hong, D. K. Bonner, Z. Poon and P. T. Hammond, *Nat. Mater.*, 2012, **11**, 316–322; (*c*) A. V. Pinheiro, D. Han, W. M. Shih and H. Yan, *Nat. Nanotechnol.*, 2011, **6**, 763–772; (*d*) J. D. Flory, C. R. Simmons, S. Lin, T. Johnson, A. Andreoni, J. Zook, G. Ghirlanda, Y. Liu, H. Yan and P. Fromme, *J. Am. Chem. Soc.*, 2014, **136**, 8283–8295.

2 N. Park, S. H. Um, H. Funabashi, J. Xu and D. Luo, *Nat. Mater.*, 2009, **8**, 432–437.

3 Z. Zhao, J. Fu, S. Dhakal, A. J. Buck, M. Liu, T. Zhang, N. W. Woodbury, Y. Liu, N. G. Walter and H. Yan, *Nat. Commun.*, 2016, **7**, 10619.

4 G. Zhu, R. Hu, Z. Zhao, Z. Chen, X. Zhang and W. Tan, *J. Am. Chem. Soc.*, 2013, **135**, 16438–16445.

5 T. Sen, A. Sebastianelli and I. J. Bruce, *J. Am. Chem. Soc.*, 2006, **128**, 7130–7131.

6 Y. Weizmann, F. Patolsky, E. Katz and I. Willner, *J. Am. Chem. Soc.*, 2003, **125**, 3452–3454.

7 (*a*) A. H. Lu, E. L. Salabas and F. Schüth, *Angew. Chem., Int. Ed.*, 2007, **46**, 1222–1244; (*b*) D. Alcantara, Y. Guo, H. Yuan, C. J. Goergen, H. H. Chen, H. Cho, D. E. Sosnovik and L. Josephson, *Angew. Chem., Int. Ed.*, 2012, **51**, 6904–6907.

8 (*a*) X. Jin, H. Li, S. Wang, N. Kong, H. Xu, Q. Fu, H. Gu and J. Ye, *Nanoscale*, 2014, **6**, 14360–14370; (*b*) C. Adams, L. L. Israel, S. Ostrovsky, A. Taylor, H. Poptani, J. P. Lellouche and D. Chari, *Adv. Healthcare Mater.*, 2016, **5**, 841–849; (*c*) A. Fu, W. Hu, L. Xu, R. J. Wilson, H. Yu, S. J. Osterfeld, S. S. Gambhir and S. X. Wang, *Angew. Chem., Int. Ed.*, 2009, **48**, 1620–1624; (*d*) H. Marie, L. Lemaire, F. Franconi, S. Lajnef, Y. M. Frapart, V. Nicolas, G. Frébourg, M. Trichet, C. Ménager and S. Lesieur, *Adv. Funct. Mater.*, 2015, **25**, 1258–1269.

9 (*a*) Y. Wang and H. Gu, *Adv. Mater.*, 2015, **27**, 576–585; (*b*) K. Cheng, D. Shen, M. T. Hensley, R. Middleton, B. Sun and W. Liu, *Nat. Commun.*, 2014, **5**, 4880.

10 A. Cavalli, M. L. Bolognesi, A. Minarini, M. Rosini, V. Tumiatti, M. Recanatini and C. J. Melchiorre, *Med. Chem.*, 2008, **51**, 347–372.

11 (*a*) T. Donnelly, W. E. Smith, K. Faulds and D. Graham, *Chem. Commun.*, 2014, **50**, 12907–12910; (*b*) J. Zheng, Y. Hu, J. Bai, C. Ma, J. Li, Y. Li, M. Shi, W. Tan and R. Yang, *Anal. Chem.*, 2014, **86**, 2205–2212; (*c*) X. Wei, T. Tian, S. Jia, Z. Zhu, Y. Ma, J. Sun, Z. Lin and C. Yang, *Anal. Chem.*, 2015, **87**, 4275–4282.

12 G. Jalani, R. Naccache, D. H. Rosenzweig, L. Haglund, F. Vetrone and M. Cerruti, *J. Am. Chem. Soc.*, 2016, **138**, 1078–1083.

13 (*a*) M. Liong, J. Lu, M. Kovochich, T. Xia, S. G. Ruehm, A. E. Nel, F. Tamanoi and J. I. Zink, *ACS Nano*, 2008, **2**, 889–896; (*b*) L. S. Lin, Z. X. Cong, J. B. Cao, K. M. Ke, Q. L. Peng, J. Gao, H. H. Yang, G. Liu and X. Chen, *ACS Nano*, 2014, **8**, 3876–3883; (*c*) L. Zhang, Y. Li, Z. Chen, L. Li, P. Saint-Cricq, C. Li, J. Lin, C. Wang, Z. Su and J. I. Zink, *Angew. Chem., Int. Ed.*, 2016, **55**, 2118–2121.

14 (*a*) L. Wang, R. Deng and J. Li, *Chem. Sci.*, 2015, **6**, 6777–6782; (*b*) G. Chen, D. Liu, C. He, T. R. Gannett, W. Lin and Y. Weizmann, *J. Am. Chem. Soc.*, 2015, **137**, 3844–3851.

15 (*a*) X. Zhang, R. Li, Y. Chen, S. S. Zhang, W. Wang and F. Li, *Chem. Sci.*, 2016, **7**, 6182–6189; (*b*) C. Russell, K. Welch, J. Jarvius, Y. Cai, R. Brucas, F. Nikolajeff, P. Svedlindh and M. Nilsson, *ACS Nano*, 2014, **8**, 1147–1153.

16 V. Bagalkot, O. C. Farokhzad, R. Langer and S. Jon, *Angew. Chem., Int. Ed.*, 2006, **45**, 8149–8152.

17 Q. Jiang, C. Song, J. Nangreave, X. Liu, L. Lin, D. Qiu, Z. G. Wang, G. Zou, X. Liang, H. Yan and B. Ding, *J. Am. Chem. Soc.*, 2012, **134**, 13396–13403.

18 D. Shangguan, Y. Li, Z. Tang, Z. C. Cao, H. W. Chen, P. Sefah, K. Mallikaratchy, C. J. Yang and W. Tan, *Proc. Natl. Acad. Sci. U. S. A.*, 2006, **103**, 11838–11843.

19 J. B. Boulé, F. Rougeon and C. Papanicolaou, *J. Biol. Chem.*, 2001, **276**, 31388–31393.

20 C. P. Leamon and J. A. Reddy, *Adv. Drug Delivery Rev.*, 2004, **56**, 1127–1141.

21 J. Yang, H. Chen, I. R. Vlahov, J. X. Cheng and P. S. Low, *Proc. Natl. Acad. Sci. U. S. A.*, 2006, **103**, 13872–13877.

22 J. B. Lee, S. Peng, D. Yang, Y. H. Roh, H. Funabashi, N. Park, E. J. Rice, L. Chen, R. Long, M. Wu and D. Luo, *Nat. Nanotechnol.*, 2012, **7**, 816–820.

23 (*a*) J. Wang, D. Ma, Q. Lu, S. Wu, G. Y. Lee, L. A. Lane, B. Li, L. Quan, Y. Wang and S. Nie, *Nanoscale*, 2015, **7**, 15185–15190; (*b*) J. Tian, L. Ding, H. J. Xu, Z. Shen, H. Ju, J. Li, L. Bao and J. S. Yu, *J. Am. Chem. Soc.*, 2013, **135**, 18850–18858.